ORIGINAL   **Open Access**

Synthesis, characterization, and investigation of optical and magnetic properties of cobalt oxide (Co$_3$O$_4$) nanoparticles

Saeed Farhadi[*], Jalil Safabakhsh and Parisa Zaringhadam

Abstract

Spinel-type cobalt oxide (Co$_3$O$_4$) nanoparticles have been easily prepared through a simple thermal decomposition route at low temperature (175°C) using carbonatotetra(ammine)cobalt(III) nitrate complex, [Co(NH$_3$)$_4$CO$_3$]NO$_3$·H$_2$O, as a new precursor. The structure and morphology of as-prepared Co$_3$O$_4$ nanoparticles were characterized by Fourier transform infrared (FT-IR) spectroscopy, X-ray diffraction (XRD), transmission electron microscopy (TEM), energy-dispersive X-ray spectroscopy (EDS), UV–vis spectroscopy, Brunauer-Emmett-Teller specific surface area measurement and magnetic measurements, and thermogravimetry/differential thermal analysis. The FT-IR, XRD, and EDS results indicated that the product was highly pure well-crystallized cubic phase of Co$_3$O$_4$. The TEM images showed that the product powder consisted of dispersive quasi-spherical particles with a narrow size distribution ranged from 6 to 16 nm and an average size around 11 nm. The magnetic measurements confirmed that the Co$_3$O$_4$ nanoparticles show a little ferromagnetic behavior which could be attributed to the uncompensated surface spins and/or finite size effects. The ferromagnetic order of the Co$_3$O$_4$ nanoparticles is raised with increasing the decomposition temperature. Using the present method, Co$_3$O$_4$ nanoparticles can be produced without the need of expensive organic solvents and complicated equipments.

Keywords: Co$_3$O$_4$ nanoparticles; Soft chemical methods; Co(III) amine complex; Thermal decomposition; Optical properties; Magnetic properties

Background

Nanometer-scale materials with the size of 1 to 100 nm have attracted considerable interest in recent years due to the departure of properties from bulk phases arising from quantum size effects [1]. Spinel-type cobalt oxide (Co$_3$O$_4$) is a technologically important material with applications in lithium ion batteries, heterogeneous catalysts, gas sensing, ceramic pigments, and electrochemical devices [2-11]. This transition metal oxide, when falling in the nanosized regime, is expected to lead to even more attractive applications in the conjunction of their traditional arena and nanotechnology.

In recent years, many efforts have been devoted to the synthesis of Co$_3$O$_4$ nanostructures with different morphologies such as nanoparticles, hollow spheres, nanorods, nanoplates, nanowires, nanotubes, and nanocubes, and nanoporous structures have been prepared [12-22].

Among them, Co$_3$O$_4$ nanoparticles have been prepared by various physical and chemical techniques such as combustion method, microwave irradiation, hydrothermal/solvothermal method, sol–gel process, chemical spray pyrolysis, sonochemical method, polyol method, and so on [23-37]. Most of these methods need some special instruments, harsh conditions, and relatively high processing temperature higher than 350°C. In addition, these methods are either time-consuming or require expensive instruments.

Among various soft chemical methods for preparing nanoscale materials, the thermal decomposition method is widely used due to the process simplicity [38-40]. This technique offers several unique advantages over other methods including easy work-up, low temperature processing, short reaction time, and production of inorganic nanomaterials with narrow size distribution. In recent years, several precursors have been used to synthesize Co$_3$O$_4$ nanoparticles via the thermal decomposition

* Correspondence: sfarhadi48@yahoo.com
Department of Chemistry, Lorestan University, Khoramabad 68135-465, Iran
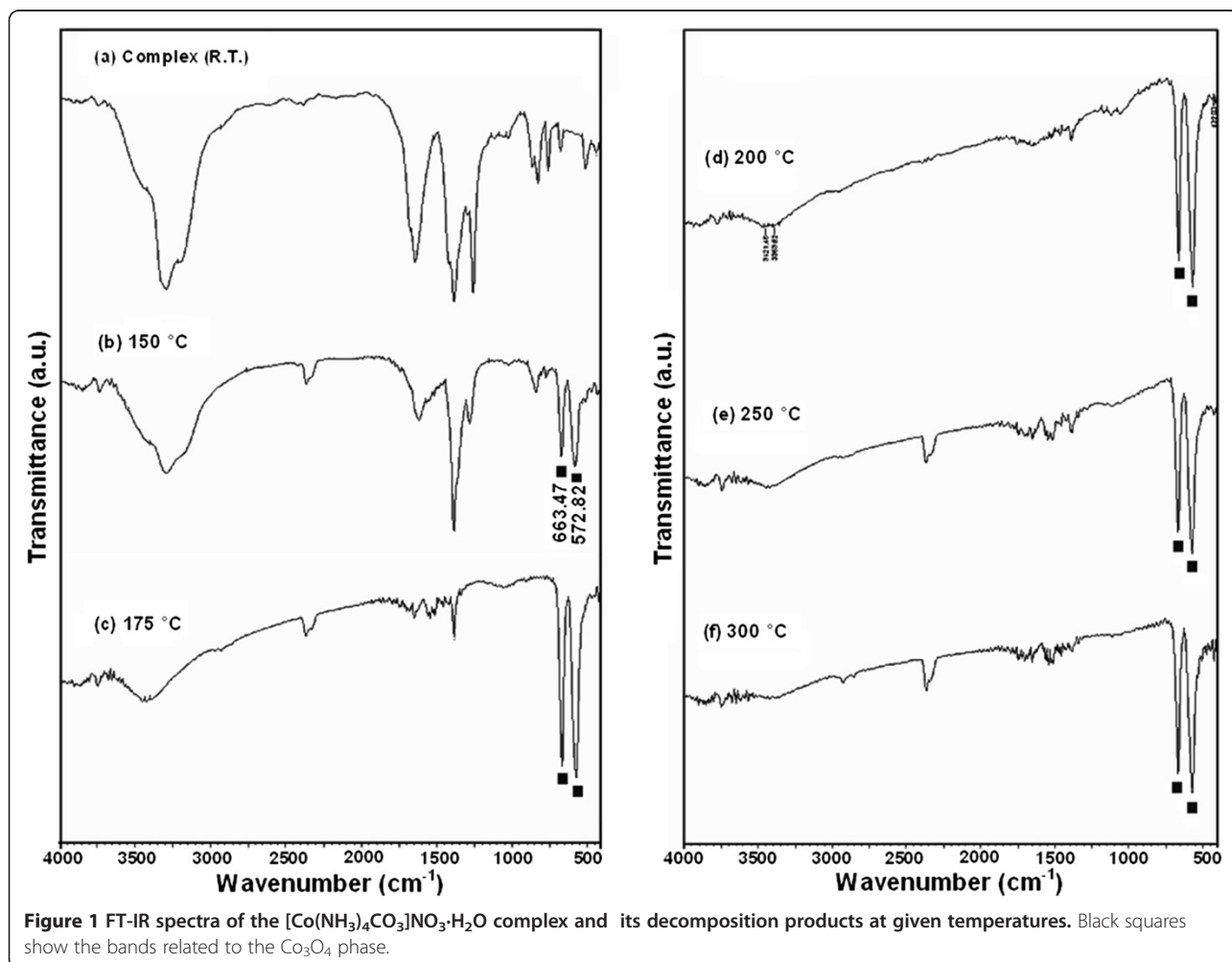
technique [41-45]. However, the most important issue in this technique is to design a precursor which would allow the synthesis of nanomaterials at a low temperature.

In this work, we wish to describe the thermal decomposition of the carbonatotetra(ammine)cobalt(III) nitrate complex, $[Co(NH_3)_4CO_3]NO_3 \cdot H_2O$, which resulted in the synthesis of Co_3O_4 nanoparticles at rather low temperature (175°C). The product was identified by various instrumental techniques such as X-ray diffraction (XRD), Fourier transform infrared (FT-IR), transmission electron microscopy (TEM), energy-dispersive X-ray spectroscopy (EDS), thermogravimetry/differential thermal analysis (TG/DTA), UV–vis spectroscopy, Brunauer-Emmett-Teller (BET) surface area measurement, and magnetic measurement. This approach provides a one-step, simple, general, and inexpensive method for the preparation of the Co_3O_4 nanoparticles.

Results and discussion

The FT-IR spectra of the $[Co(NH_3)_4CO_3]NO_3 \cdot H_2O$ complex and its decomposition products at different temperatures are shown in Figure 1. For the complex (Figure 1, curve a), the characteristic stretching bands of NH_3, CO_3, and NO_3 groups are observed at approximately 3,250 to 3,500, 1,600, and 1,350 cm^{-1}, respectively [46]. As shown in Figure 1, curve b, the intensity of these bands decreases when the complex is heated at 150°C. At this temperature, there are two small absorption bands (black square) at about 663.47 and 572.82 cm^{-1}, providing clear evidence for the presence of the crystalline Co_3O_4 [12]. This observation confirms that the formation of Co_3O_4 nanocrystals begins at approximately 150°C. As can be clearly seen in Figure 1, curve c, with increasing the decomposition temperature to 175°C, only two strong bands assigned to the Co-O stretching of the cubic Co_3O_4 structure are observed [47]. As shown in Figure 1, curves d,e,f, FT-IR spectra of the samples that were decomposed in the 200°C to 300°C range show only the bands related to the Co_3O_4 without obvious changes. It is noted that the bands at approximately 3,550 and 1,650 cm^{-1} in the FT-IR spectrum of some samples should be assigned to the stretching and bending vibrations of the water molecules
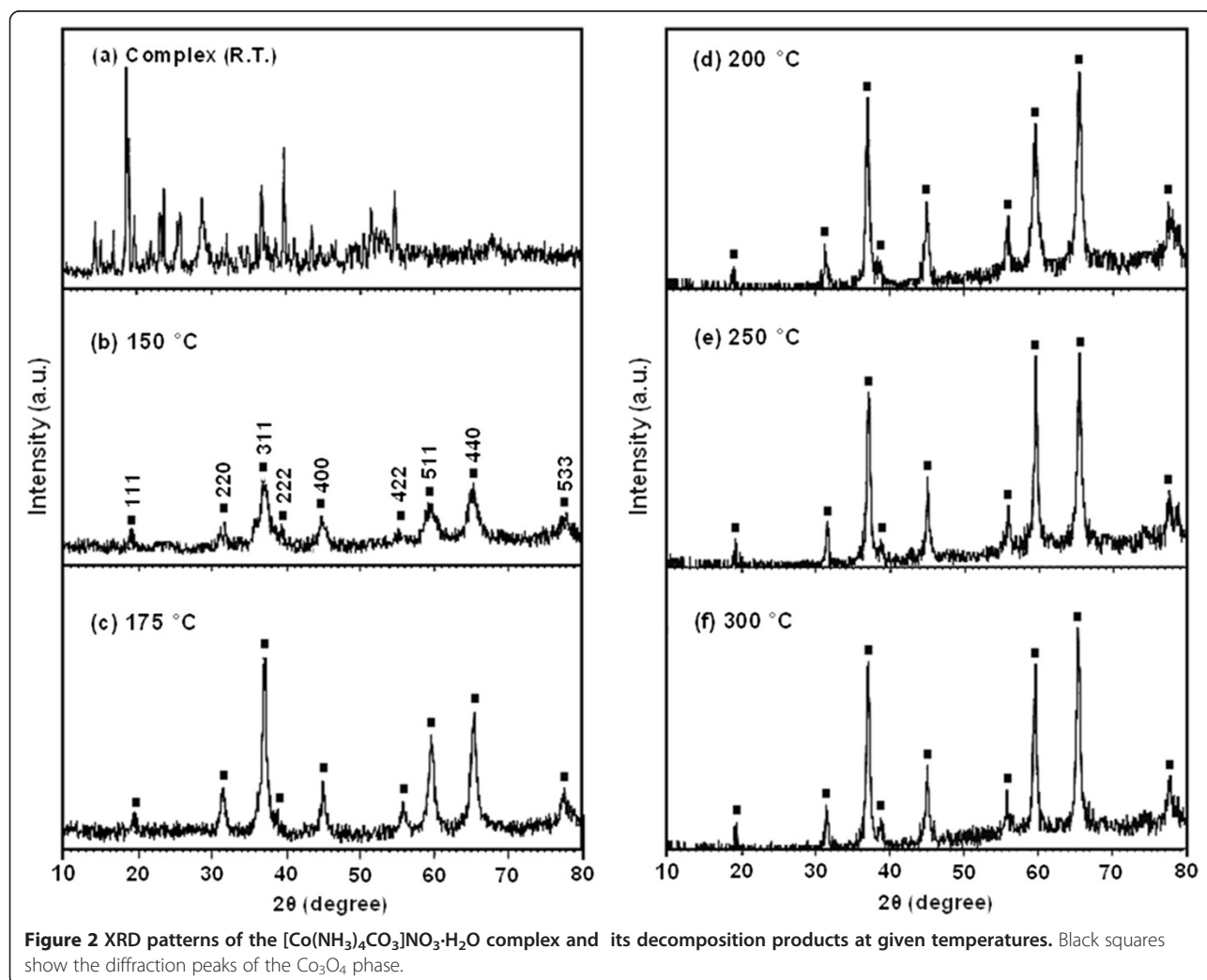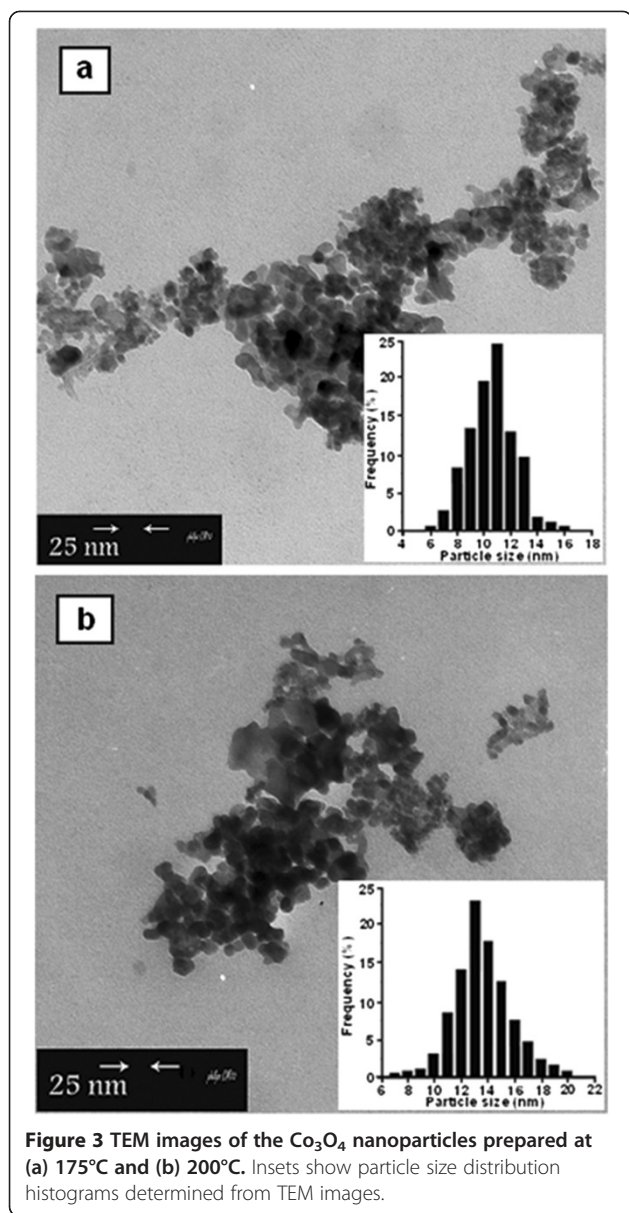

Figure 1 FT-IR spectra of the $[Co(NH_3)_4CO_3]NO_3 \cdot H_2O$ complex and its decomposition products at given temperatures. Black squares show the bands related to the Co_3O_4 phase.

absorbed by the samples or KBr. Also, there is a tiny band at approximately 2,360 cm^{-1} on the spectrum of some samples due to the presence of atmospheric CO_2.

The XRD patterns of the $[Co(NH_3)_4CO_3]NO_3 \cdot H_2O$ complex and its decomposition products at various temperatures are shown in Figure 2. Figure 2a shows the XRD pattern of $Co(NH_3)_4CO_3]NO_3 \cdot H_2O$ precursor. All diffraction peaks appeared in this pattern match very well with those reported in literature for the pure $[Co(NH_3)_4CO_3]NO_3 \cdot H_2O$ (JCPDS 50–1674). As can be seen in Figure 2b, all diffraction peaks related to $[Co(NH_3)_4CO_3]NO_3 \cdot H_2O$ disappeared at 150°C and new broad and weak peaks with 2θ values at 19.50°, 31.37°, 37.02°, 39.10°, 44.97°, 55.84°, 59.58°, 65.46°, and 77.62° appeared. These diffraction peaks can be indexed to the crystalline cubic phase Co_3O_4 with lattice constants of a = 8.076 Å and a space group of Fd3 m, which are in agreement with the reported values (JCPDS card no. 76–1802). As shown in Figure 2c, the intensity of the characteristic peaks of the Co_3O_4 phase increases markedly as
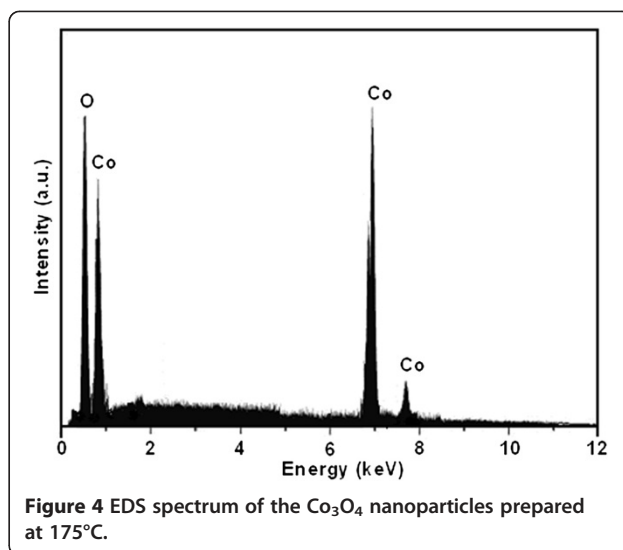
the temperature increases to 175°C, confirming the complete formation of the Co_3O_4 phase in good agreement with the FT-IR result. No characteristic peaks of other impurity phases have been detected, indicating that the final product is of high purity. The considerable broadening of the diffraction peaks demonstrates the nanometric character of the particles. The average size of particles prepared was estimated to be about 11.5 nm by the Debye-Scherrer equation [48]: $D_{XRD} = 0.9\lambda/(\beta cos\theta)$ where D_{XRD} is the average crystalline size, λ is the wavelength of CuKα, β is the full width at half maximum of the diffraction peak, and θ is the Bragg's angle. As we can see in Figure 2d, e,f, no new phase is observed when the decomposition temperature increases to 200°C, 250°C, and then 300°C, but the width of the Co_3O_4 peaks decreases because of crystallite growth. Further, the increase in the sharpness of peaks with increasing temperature indicates the well crystallization of the product.

The size and shape of the Co_3O_4 particles prepared by the thermal decomposition of the $[Co(NH_3)_4CO_3]$

Figure 2 XRD patterns of the $[Co(NH_3)_4CO_3]NO_3 \cdot H_2O$ complex and its decomposition products at given temperatures. Black squares show the diffraction peaks of the Co_3O_4 phase.

Figure 3 TEM images of the Co$_3$O$_4$ nanoparticles prepared at (a) 175°C and (b) 200°C. Insets show particle size distribution histograms determined from TEM images.

Figure 4 EDS spectrum of the Co$_3$O$_4$ nanoparticles prepared at 175°C.

insets of Figure 3. The inset of Figure 3a shows the particle size distribution of the Co$_3$O$_4$ nanoparticles prepared at 175°C. It can be seen that the particles possess a narrow size distribution in the range of 6 to 16 nm, and the mean particle diameter is approximately 11 nm. Actually, the mean particle size determined by TEM is very close to the average particle size calculated by the Debye-Scherrer formula from the XRD pattern. The particle size distribution was also presented for the Co$_3$O$_4$ nanoparticles prepared at 200°C in the inset of Figure 3b. The size of particles is in the range of 7 to 20 nm with an average particle size of around 13 nm. This value is slightly greater than that of the Co$_3$O$_4$ nanoparticles prepared at 175°C probably due to the crystallite growth at the higher temperature.

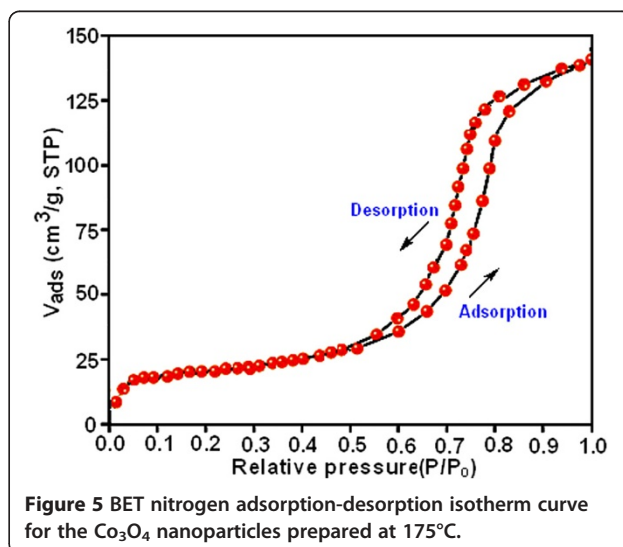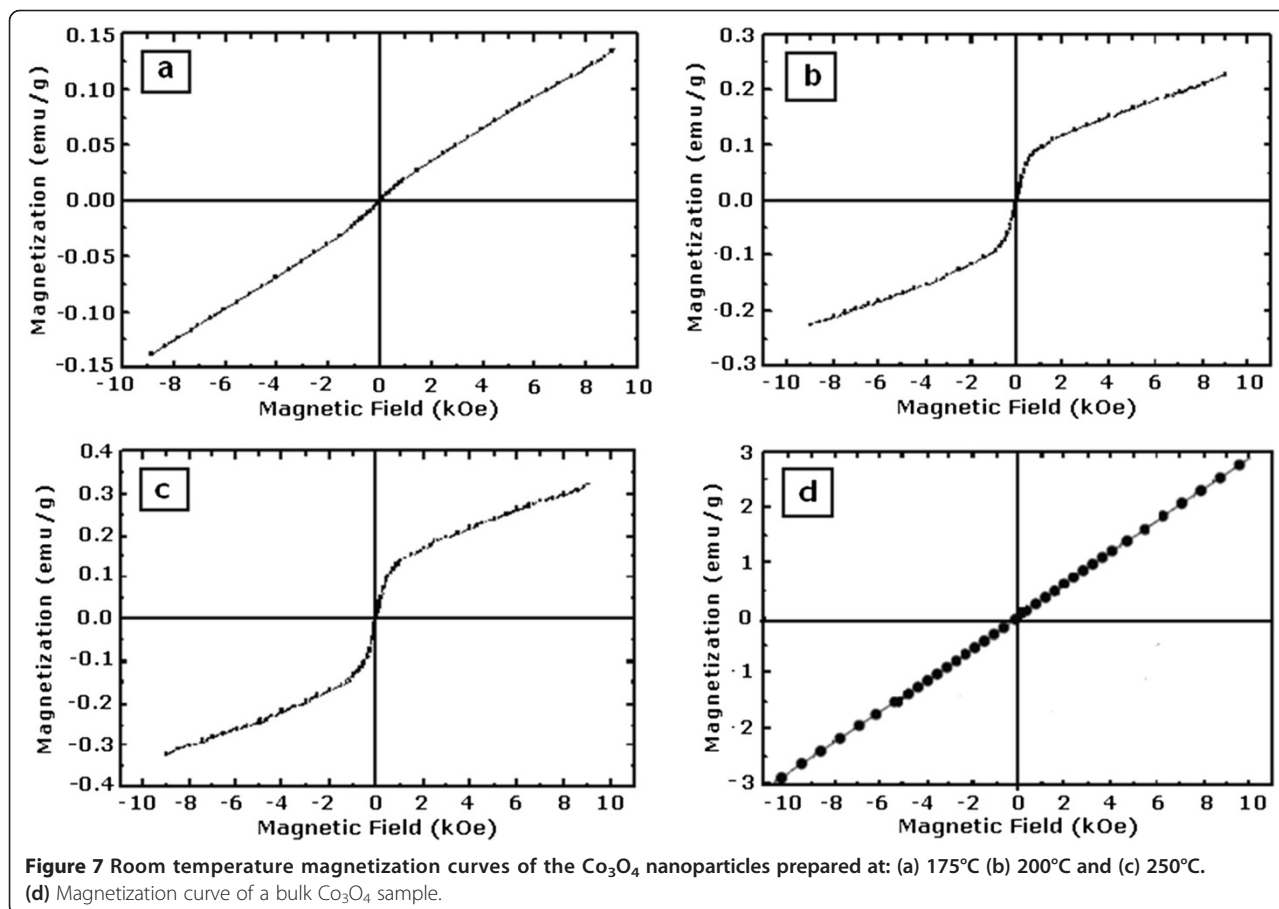The EDS analysis was employed to determine the composition of the product prepared at 175°C. As shown

NO$_3$·H$_2$O complex at 175°C and also at 200°C were investigated by TEM, as shown in Figure 3a,b. In both cases, the TEM analysis revealed that the samples were formed from extremely fine particles with the sizes of less than 20 nm. It is evident that the particles have uniform size, a homogeneous sphere-like morphology and a narrow size distribution. From the TEM images, it could be concluded that this preparation method is appropriate to obtain the Co$_3$O$_4$ nanoparticles with very small size. The size distribution of the Co$_3$O$_4$ nanoparticles has also been investigated from the particles visualized under TEM analysis. The particle size histograms were determined by counting more than 100 particles in randomly selected regions on the TEM copper grid. The histograms based on TEM analysis are shown in the

Figure 5 BET nitrogen adsorption-desorption isotherm curve for the Co$_3$O$_4$ nanoparticles prepared at 175°C.

Figure 6 UV–vis spectrum and $(Ahv)^2 - hv$ curve (inset) of the Co_3O_4 nanoparticles prepared at 175°C.
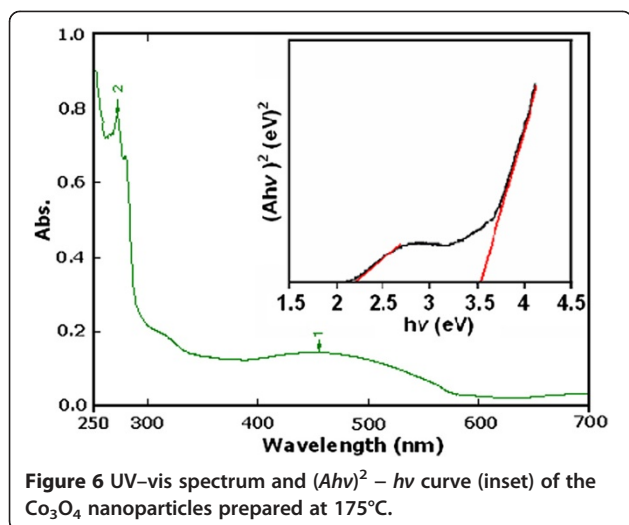
in Figure 4, only cobalt and oxygen elements existed in the product with a Co/O atomic ratio of about 3:3.97 which is consistent with the theoretical value of Co_3O_4. No other elements can be detected, indicating the high purity of the Co_3O_4 nanoparticles.

BET surface area measurements were also made on the Co_3O_4 nanoparticles prepared at 175°C. Figure 5 shows N_2 adsorption-desorption which is close to type IV of the IUPAC classification with an evident hysteresis loop in the 0.5 to 1.0 range, suggesting that the sample under study is basically mesoporous. The specific surface area of the sample calculated by the BET method is 73.70 m^2 g^{-1}. The relatively high specific surface area of the product is related to the nanometric size of its particles. Assuming that the Co_3O_4 nanoparticles are almost spherical, as confirmed by TEM, the surface area can be used to estimate the particle size according to the equation $D_{BET} = 6000/(\rho \times S_{BET})$, where D_{BET} is the diameter of a spherical particle (in nm), ρ is the theoretical density of Co_3O_4 (6.08 g cm^{-3}), and S_{BET} is the specific surface area of the Co_3O_4 powder in meter squared per gram. The particle size calculated from the surface area data is approximately 13.4 nm, which is in good agreement with the XRD and TEM results.

Optical absorption properties of the Co_3O_4 nanoparticles prepared at 175°C were investigated at room temperature by UV–vis spectroscopy. Figure 6 shows the absorbance spectrum of the Co_3O_4 sample with two absorption bands

Figure 7 Room temperature magnetization curves of the Co_3O_4 nanoparticles prepared at: (a) 175°C (b) 200°C and (c) 250°C.
(d) Magnetization curve of a bulk Co_3O_4 sample.

in 250 to 350 and 400 to 580 nm wavelength ranges. The first band can be assigned to the $O^{2-} \rightarrow Co^{2+}$ charge transfer process while the second one to the $O^{2-} \rightarrow Co^{3+}$ charge transfer [49]. Co_3O_4 is a p-type semiconductor, and the absorption band gap (E_g) can be determined by the following equation [24]: $(Ah\nu)^2 = K (h\nu - E_g)$, where $h\nu$ is the photon energy (eV), A is the absorption coefficient, K is a constant, and E_g is the band gap. The band gap can be estimated by extrapolating the linear region in the plot of $(Ah\nu)^2$ versus photon energy as shown in the inset of Figure 6. Two absorption peaks give two E_g values for the product, 3.55 and 2.2 eV. As it has been reported in the literatures [50], the E_g values of Co_3O_4 nanoparticles prepared in this study are greater than those of the bulk Co_3O_4 (E_g = 3.17 and 1.77 eV, respectively). The increase in the band gaps can be related to the quantum confinement effects and/or small size effects of the Co_3O_4 nanoparticles [33,50].

The magnetic measurements for the Co_3O_4 samples prepared at different temperatures were carried out at room temperature. As shown in Figure 7a, the magnetization curve for the Co_3O_4 nanoparticles prepared at 175°C exhibits a weak ferromagnetic behavior with a saturation magnetization of 0.137 emu g^{-1} at the maximum field of 9 kOe applied while the magnetization curves for the Co_3O_4 samples prepared at 200°C and 250°C in the same figure (Figure 7b,c) display higher ferromagnetic properties with saturation magnetization values of 0.225 and 0.325 emu g^{-1} at the applied field of 9 kOe, respectively. To confirm that the ferromagnetic behavior originates from the nanoparticles, this measurement was also conducted on a bulk sample. As shown in Figure 7d, the curve exhibits an antiferromagnetic behavior. The ferromagnetic behavior of the nanoparticles can be explained as follows: bulk Co_3O_4 has a normal spinel structure with antiferromagnetic exchange between ions which occupy the tetrahedral and octahedral sites [51]. It has zero net magnetization owing to the complete compensation of sublattice magnetizations. Hence, the change from an antiferromagnetic state for bulk Co_3O_4 to a weakly ferromagnetic state for the Co_3O_4 nanoparticles can be ascribed to the uncompensated surface spins and/or finite size effects [11,41,52,53]. It is well known that the magnetic properties of nanomaterials are strongly dependent on the shape and sizes of their particles, crystallinity, magnetization direction, and so on.

In order to obtain further insight into the nature of the reactions involved in the decomposition pathway of the complex, its thermal behavior was investigated by TG/DTA. Figure 8 shows TG/DTA curves recorded for $[Co(NH_3)_4CO_3]NO_3 \cdot H_2O$ in the 25°C to 600°C temperature range. The TG curve shows that the decomposition of complex proceeds in three stages. The first stage occurred at about 95°C to 110°C and shows
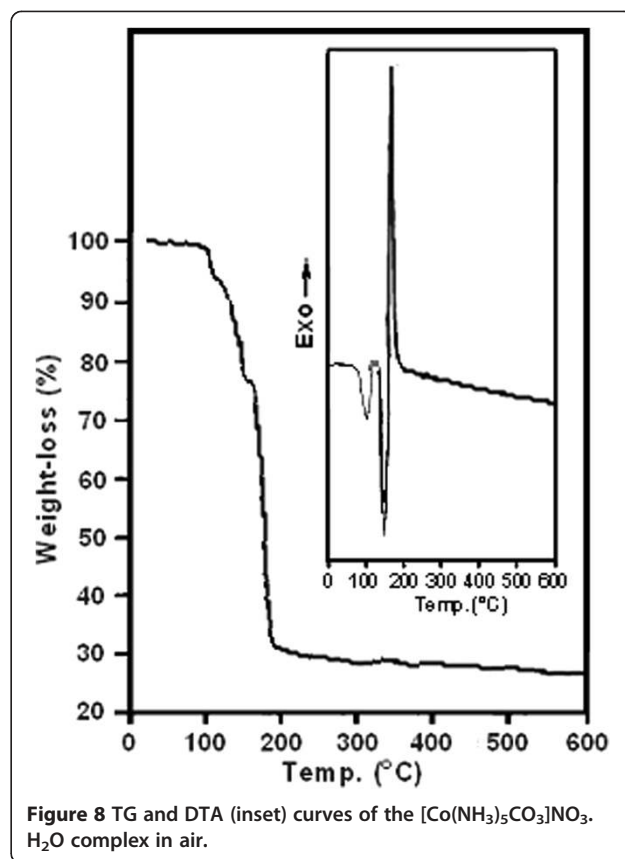

Figure 8 TG and DTA (inset) curves of the $[Co(NH_3)_5CO_3]NO_3$. H_2O complex in air.

6.68% weight loss which is consistent with the theoretical value of 6.75% caused by the loss of 1 mol of H_2O per mole of the complex. The second stage occurs at approximately 135°C to 150°C and shows a 16.75% weight loss, which is consistent with the theoretical value of 16.50% caused by the loss of 1 mol of CO_2 per mole of the complex. In the third stage, an extensive weight loss is observed in the range of 160°C to 175°C, which related to the decomposition of the residue complex. Above 175°C, the weight remained constant, confirming the complete decomposition of the complex. The weight loss of all steps that is about 70% is consistent with the theoretical value (70.10%) calculated for the formation of Co_3O_4 from the complex. The DTA curve for the $[Co(NH_3)_4CO_3]NO_3 \cdot H_2O$ complex as shown in the inset of Figure 8 gave three characteristic peaks in consistent with TG data. The small endothermic peaks at about 100°C can be explained by freeing one H_2O molecule. The decomposition of the dehydrated complex was confirmed by one endothermic peak at about 150°C which is immediately followed by a sharp exothermic peak at about 175°C. The endothermic peak at 150°C can be related to the decomposition of unstable bidentate

carbonato ligand, and the sharp exothermic peak can be explained by the explosive decomposition of the complex via a redox process taking place between the NH_3 ligands as the reductants and NO_3^- and/or O_2 as oxidants. According to the TG/DTG data, the decomposition reactions of the complex can be written as follows:

- Step 1: $[Co(NH_3)_4CO_3]NO_3 \cdot H_2O(s) \rightarrow [Co(NH_3)_4CO_3]NO_3$ (s) + H_2O (g)
- Step 2: $[Co(NH_3)_4CO_3]NO_3$ (s) $\rightarrow [Co(NH_3)_4O]NO_3$ (s) + CO_2 (g)
- Step 3: $[Co(NH_3)_4O]NO_3$ (s) + $13/3 O_2 \rightarrow 1/3 Co_3O_4$ (s) + $6H_2O$ (g) + NO (g) (or NO_2) + 2 N_2 (g)

Conclusions

In summary, pure and nanosized Co_3O_4 particles with an average particle size of 11 nm were successfully synthesized by the thermal decomposition of the $[Co(NH_3)_4CO_3]NO_3 \cdot H_2O$ complex as a new precursor at 175°C. Co_3O_4 nanoparticles are probably formed via the elimination of H_2O and CO_2 molecules and then explosive redox reaction between the NH_3 ligands as the reducing agent and the NO_3^- ions as the oxidizing agent. By this method, uniform and sphere-like Co_3O_4 nanoparticles with a narrow size distribution and a weak ferromagnetic behavior can be obtained. The optical absorption band gaps of the Co_3O_4 nanoparticles were estimated to be approximately 2.20 and 3.55 eV, which are blue shifted in comparison with previously reported values. This method is simple, low cost, safe, and suitable for the industrial production of high-purity Co_3O_4 nanoparticles for various applications.

Methods

Materials

All materials were of analytical grade and obtained from Merck Company, Merck KGaA, Darmstadt, Germany. Solvents used throughout the reactions were of high purity and used without further purification.

Synthesis of Co_3O_4 nanoparticles

The precursor complex, $[Co(NH_3)_4CO_3]NO_3 \cdot H_2O$, was synthesized according to the literature method [54]. To prepare Co_3O_4 nanoparticles, an appropriate amount of the precursor complex (1 to 2 g) was added to a porcelain crucible and then was placed in an electric furnace. The sample was heated at the rate of 10°C min^{-1} from room temperature to 150°C in an air atmosphere and then was maintained at this temperature for 1 h. Similar experiments were performed for the samples decomposed in the range of 175°C to 300°C. The decomposition products of the complex at various temperatures were cooled to room temperature and collected for the characterization.

Characterization

The XRD patterns were recorded on a Rigaku D-max C III, X-ray diffractometer (Rigaku Corporation, Shibuya-ku, Japan) using Ni-filtered CuKα radiation (λ = 1.5406 Å) to determine the phases present in the decomposed samples. Infrared spectra were recorded on a Shimadzu system FT-IR 8400S spectrophotometer (Shimadzu Corporation, Kyoto, Japan) using KBr pellets. The optical absorption spectrum was recorded on a Shimadzu 1650PC UV–vis spectrophotometer in the 250 to 700 nm wavelength range at room temperature. The sample for UV–vis studies was well dispersed in distilled water to form a homogeneous suspension by sonication for 25 min. The particle size was determined by a transmission electron microscope (Philips CM10, Philips, Amsterdam, The Netherlands) equipped with a link EDS analyzer. The powders were ultrasonicated in ethanol, and a drop of the suspension was dried on a carbon-coated copper microgrid for the TEM measurements. The specific surface area of the product was measured by the BET method using an N_2 adsorption-desorption isotherm carried out at –196°C on a surface area analyzer (Micromeritics ASAP 2010, Micromeritics, Norcross, GA, USA). Before each measurement, the sample was degassed at 150°C for 2 h. Magnetic measurements were carried out at room temperature using a vibrating sample magnetometer (Meghnatis Daghigh Kavir Co. Kashan, Iran). The thermal behavior of the precursor complex was studied using a Netzsch STA 409 PC/PG thermal analyzer (Netzsch, Burlington, MA, USA) at a heating rate of 5°C min^{-1} in air.

Competing interests

The authors declare that they have no competing interests.

Authors' contributions

SF proposed the idea of the study, revised the manuscript critically, and gave final approval for submission. JS was involved in the synthesis and the physicochemical characterization of the Co_3O_4 nanoparticles and early drafted the manuscript. PZ was involved in the analysis and interpretation of spectral and thermal analysis data. All authors read and approved the final manuscript.

Authors' information

SF received his BSc degree in Chemistry from Shahid Chamran University in 1991, his MSc degree in Inorganic Chemistry from Tehran University in 1994, and his Ph. D in Inorganic Chemistry from Isfahan University, Iran, in 2000. He is now a professor in inorganic chemistry and the head of the Chemistry Department at Lorestan University, Iran. His research area interests have concentrated on synthesis and characterization of metal and metal oxide nanostructures and their catalytic applications. JS got his BSc in Chemistry in

2009 from the Faculty of Science, Kashan University, Iran. He obtained his MSc in inorganic chemistry in 2012 with the thesis entitled 'Low-temperature synthesis of Co_3O_4 nanoparticles from thermal decomposition of the [Co(NH$_3$)$_4$(L)](NO$_3$)$_n$ complexes (L = CO$_3$, NO$_3$, H$_2$O; n = 1–3) and their characterization' from the Faculty of Science, Lorestan University, Iran. PZ obtained her BSc and MSc degrees in Chemistry from the Faculty of Science, Lorestan University, Iran, in 2003 and 2006, respectively. During her MSc course, she has been involved in synthesizing mullite and magnesium aluminate spinel nanopowders by sol–gel process.

References
1. Klabunde, KJ, Richards, RM: Nanoscale Materials in Chemistry, 2nd edn. Wiley, New York (2012)
2. Mate, VR, Shirai, M, Rode, CV: Heterogeneous Co_3O_4 catalyst for selective oxidation of aqueous veratryl alcohol using molecular oxygen. Catal Commun 33, 66–69 (2013)
3. Warang, T, Patel, N, Santini, A, Bazzanella, N, Kale, A, Miotello, A: Pulsed laser deposition of Co_3O_4 nanoparticles assembled coating: role of substrate temperature to tailor disordered to crystalline phase and related photocatalytic activity in degradation of methylene blue. Appl. Catal. A: Gen. 423–424, 21–27 (2012)
4. Casas-Cabanas, M, Binotto, G, Larcher, D, Lecup, A, Giordani, V, Tarascon, JM: Defect chemistry and catalytic activity of nanosized Co_3O_4. Chem Mater 21, 1939–1947 (2009)
5. Askarinejad, A, Bagherzadeh, M, Morsali, A: Catalytic performance of Mn_3O_4 and Co_3O_4 nanocrystals prepared by sonochemical method in epoxidation of styrene and cyclooctene. Appl. Surface Sci. 256, 6678–6682 (2010)
6. Lou, XW, Deng, D, Lee, JY, Feng, J, Archer, LA: Self-supported formation of needlelike Co_3O_4 nanotubes and their application as lithium-ion battery electrodes. Adv Mater 20, 258–262 (2008)
7. Chou, S-L, Wang, J-Z, Liu, H-K, Dou, S-X: Electrochemical deposition of porous Co_3O_4 nanostructured thin film for lithium-ion battery. J Power Sources 182, 359–364 (2008)
8. Li, YG, Tan, B, Wu, YY: Mesoporous Co_3O_4 nanowire arrays for lithium ion batteries with high capacity and rate capacity. Nano Lett 8, 265–270 (2008)
9. Li, W-Y, Xu, L-N, Chen, J: Co_3O_4 nanomaterials in lithium-ion batteries and gas sensors. Adv Funct Mater 15, 851–857 (2005)
10. Sugimoto, T, Matijevic, E: Colloidal cobalt hydrous oxides, preparation and properties of monodispersed. Co_3O_4. J Inorg Nucl Chem 41, 165–172 (1979)
11. Makhlouf, SA: Magnetic properties of Co_3O_4 nanoparticles. J Magn Magn Mater 246, 184–190 (2002)
12. Sun, L, Li, H, Ren, L, Hu, C: Synthesis of Co_3O_4 nanostructures using a solvothermal approach. Solid State Sci 11, 108–112 (2009)
13. Chen, Y, Zhang, Y, Fu, S: Synthesis and characterization of Co_3O_4 hollow spheres. Mater Lett 61, 701–705 (2007)
14. Lai, T, Lai, Y, Lee, C, Shu, Y, Wang, C: Microwave-assisted rapid fabrication of Co_3O_4 nanorods and application to the degradation of phenol. Catal Today 131, 105–110 (2008)
15. Wang, WW, Zhu, YJ: Microwave-assisted synthesis of cobalt oxalate nanorods and their thermal conversion to Co_3O_4 rods. Mater Res Bull 40, 1929–1935 (2005)
16. Li, L, Chu, Y, Liu, Y, Song, JL, Wang, D, Du, XW: A facile hydrothermal route to synthesize novel Co_3O_4 nanoplates. Mater Lett 62, 1507–1510 (2008)
17. Du, J, Chai, L, Wang, G, Li, K, Qian, Y: Controlled synthesis of one-dimensional single-crystal Co_3O_4 nanowires. Aust J Chem 61, 153–158 (2008)
18. Wang, RM, Liu, CM, Zhang, HZ, Chen, CP, Guo, L, Xu, HB, Yang, SH: Porous nanotubes of Co_3O_4: synthesis, characterization and magnetic properties. Appl Phys Lett 85, 2080–2082 (2004)
19. Li, Y, Zhao, J, Dan, Y, Ma, D, Zhao, Y, Hou, S, Lin, H, Wang, Z: Low temperature aqueous synthesis of highly dispersed Co_3O_4 nanocubes and their electrocatalytic activity studies. Chem Eng J 166, 428–434 (2011)
20. Sun, H, Ahmad, M, Zhu, J: Morphology-controlled synthesis of Co_3O_4 porous nanostructures for the application as lithium-ion battery electrode. Electrochim Acta 89, 199–205 (2013)
21. Ren, M, Yuan, S, Su, L, Zhou, Z: Chrysanthemum-like Co_3O_4 architectures: hydrothermal synthesis and lithium storage performances. Solid State Sci 14, 451–455 (2012)
22. Yang, LX, Zhu, YJ, Li, L, Zhang, L, Tong, H, Wang, WW: A facile hydrothermal route to flower-like cobalt hydroxide and oxide. Eur J Inorg Chem 23, 4787–4792 (2006)
23. Jiu, J, Ge, Y, Li, X, Nie, L: Preparation of Co_3O_4 nanoparticles by a polymer combustion route. Mater Lett 54, 260–263 (2002)
24. Gu, F, Li, C, Hu, Y, Zhang, L: Synthesis and optical characterization of Co_3O_4 nanocrystals via a facile combustion method. J. Cryst. Growth 304, 369–373 (2007)
25. Gardey-Merino, MC, Palermo, M, Belda, R, Fernández De Rapp, ME, Lascalea, GE, Vázquez, PG: Combustion synthesis of Co_3O_4 nanoparticles: fuel ratio effect on the physical properties of the resulting powders. Proced. Mater. Sci 1, 588–593 (2012)
26. Ai, L-H, Jiang, J: Rapid synthesis of nanocrystalline Co_3O_4 by a microwave-assisted combustion method. Powder Tech. 195, 11–14 (2009)
27. Li, L, Ren, J: Rapid preparation of spinel Co_3O_4 nanocrystals in aqueous phase by microwave irradiation. Mater Res Bull 41, 2286–2290 (2006)
28. Bhatt, AS, Bhat, DK, Tai, C-W, Santosh, MS: Microwave-assisted synthesis and magnetic studies of cobalt oxide nanoparticles. Mater Chem Phys 125, 347–350 (2011)
29. Ma, J, Zhang, S, Liu, W, Zhao, Y: Facile preparation of Co_3O_4 nanocrystals via a solvothermal process directly from common Co_2O_3 powder. J Alloys Compd 490, 647–651 (2010)
30. Lester, E, Aksomaityte, G, Li, J, Gomez, S, Gonzalez-Gonzalez, J, Poliakoff, M: Controlled continuous hydrothermal synthesis of cobalt oxide (Co_3O_4) nanoparticles Prog. Cryst. Growth Charact. Mater. 58, 3–13 (2012)
31. Baydi, ME, Poillerat, G, Rehspringer, JL, Gautier, JL, Koenig, JF, Chartier, P: A sol–gel route for the preparation of Co_3O_4 catalyst for oxygen electrocatalysis in alkaline medium. J. Solid State Chem. 109, 281–288 (1994)
32. Kim, DY, Ju, SH, Koo, HY, Hong, SK, Kangf, YC: Synthesis of nanosized Co_3O_4 particles by spray pyrolysis. J Alloys Compd 417, 254–258 (2006)
33. Kumar, RV, Diamant, Y, Gedanken, A: Sonochemical synthesis and characterization of nanometer-size transition metal oxides from metal acetates. Chem Mater 12, 2301–2305 (2000)
34. Wang, X, Chen, XY, Gao, LS, Zheng, HG, Zhang, Z, Qian, YT: One-dimensional arrays of Co_3O_4 nanoparticles: synthesis, characterization, and optical and electrochemical properties. J Phys Chem B 108, 16401–16404 (2004)
35. Fan, S, Liu, X, Li, Y, Yan, E, Wang, C, Liu, J, Zhang, Y: Non-aqueous synthesis of crystalline Co_3O_4 nanoparticles for lithium-ionbatteries. Mater Lett 91, 291–293 (2013)
36. Jiang, J, Li, L: Synthesis of sphere-like Co_3O_4 nanocrystals via a simple polyol route. Mater Lett 61, 4894–4896 (2007)
37. Zou, D, Xu, C, Luo, H, Wang, L, Ying, T: Synthesis of Co_3O_4 nanoparticles via an ionic liquid-assisted methodology at room temperature. Mater Lett 62, 1976–1978 (2008)
38. Traversa, E, Sakamoto, M, Sadaoka, Y: A chemical route for the preparation of nanosized rare earth Perovskite-type oxides for electroceramic applications. Part Sci Technol 16, 185–214 (1998)
39. Farhadi, S, Rashidi, N: Preparation and characterization of pure single-phase $BiFeO_3$ nanoparticles through thermal decomposition of the heteronuclear Bi[Fe(CN)$_6$] · 5H$_2$O complex. Polyhedron 29, 2959–2965 (2010)
40. Farhadi, S, Roostaei-Zaniyani, Z: Simple and low-temperature synthesis of NiO nanoparticles through solid-state thermal decomposition of the hexa(ammine) Ni(II) nitrate, [Ni(NH$_3$)$_6$](NO$_3$)$_2$, complex. Polyhedron 30, 1244–1249 (2011)
41. Mohandes, F, Davar, F, Salavati-Niasari, M: Preparation of Co_3O_4 nanoparticles by nonhydrolytic thermolysis of [Co(Pht)(H$_2$O)]$_n$ polymers. J Magn Magn Mater 322, 872–877 (2010)
42. Ren, L, Wang, P, Han, Y, Hu, C, Wei, B: Synthesis of CoC_2O_4 · 2H$_2$O nanorods and their thermal decomposition to Co_3O_4 nanoparticles. Mater. Phys. Lett. 476, 78–83 (2009)
43. Thangavelu, K, Parameswari, K, Kuppusamy, K, Haldorai, Y: A simple and facile method to synthesize Co_3O_4 nanoparticles from metal benzoate dihydrazinate complex as a precursor. Mater Lett 65, 1482–1484 (2011)
44. Salavati-Niasari, M, Khansari, A, Davar, F: Synthesis and characterization of cobalt oxide nanoparticles by thermal treatment process. Inorg Chim Acta 362, 4937–4942 (2009)

45. Farhadi, S, Pourzare, K: Simple and low-temperature preparation of Co_3O_4 sphere-like nanoparticles via solid-state thermolysis of the $[Co(NH_3)_6](NO_3)_3$ complex. Mater Res Bull **47**, 1550–1556 (2012)

46. Nakamoto, K: Infrared and Raman Spectra of Inorganic and Coordination Compounds. Part B: Applications in Coordination, Organometallic, and Bioinorganic Chemistry, 6th edition, Wiley, New York (2009)

47. Pejova, B, Isahi, A, Najdoski, M: Fabrication and characterization of nanocrystalline cobalt oxide thin films. Mater Res Bull **36**, 161–170 (2001)

48. Klug, HP, Alexander, LE: X-ray Diffraction Procedures, 2nd edn. Wiley, New York (1964)

49. He, T, Chen, DR, Jiao, XL, Wang, YL, Duan, YZ: Solubility-controlled synthesis of high-quality Co_3O_4 nanocrystals. Chem Mater **17**, 4023–4030 (2005)

50. Gulino, A, Dapporto, P, Rossi, P, Fragala, I: A novel self-liquid MOCVD precursor for Co_3O_4 thin films. Chem Mater **15**, 3748–3752 (2003)

51. Ichiyanagi, Y, Kimishima, Y, Yamada, S: Magnetic study on Co_3O_4 nanoparticles. J Magn Magn Mater **272–276**, e1245–e1246 (2004)

52. Kodama, RH, Makhlouf, SA, Berkowitz, AE: Growth mechanism and magnon excitation in NiO nanowalls. Phys Rev Lett **79**, 1393–1396 (1997)

53. Ozkaya, T, Baykal, A, Toprak, MS, Koseoglu, Y, Durmus, Z: Reflux synthesis of Co_3O_4 nanoparticles and its magnetic characterization. J Magn Magn Mater **321**, 2145–2149 (2009)

54. Schlessinger, G: Synthesis of carbonatotetra(ammine)cobalt(III) nitrate. Inorg Synth **6**, 173–175 (1960)